Paper No. 285. (quote when citing this article)
Eleventh World Conference on Earthquake Engineering
ISBN: 0 08 042822 3

STRUCTURE - ELEVATOR SYSTEMS UNDER EARTHQUAKE EXCITATION

A. RUTENBERG, R. LEVY, F. SEGAL and E. MARIANCHIK

Department of Civil Engineering, Technion - Israel Institute of Technology, Technion City, Haifa 32000, ISRAEL.

ABSTRACT

This paper studies the seismic response of structure-elevator systems. The structure-elevator counterweight system is modeled as a coupled dynamic system where the structure is represented by six flexural cantilever modes (i.e. three for each of two horizontal axes), the counterweight by four degrees of freedom (two in each direction) and the dynamic interaction by a nonlinear contact element with air gaps, viscous damper, Coulomb friction and location dependent variable stiffness springs (guide rails). Nonlinear dynamic analyses were carried out using step-by-step integration of the resulting, twelve, first order differential equations. A parametric study: (*i*) Introduces the effects of vertical velocity. (*ii*) Introduces the effect of real earthquake time histories considering bidirectional excitation on the response of elevator-counterweight systems. (*iii*) Constructs design curves and compares them to the US ASME A17.1-1990 Elevator Code.

KEYWORDS

Earthquake Resistant Design; Elevators; Guide rails; Counterweight Derailment.

INTRODUCTION

Elevators are an essential transportation means for the proper functioning of buildings. The 1964 Alaska (Ayers *et al.*, 1973), the 1971 San Fernando (Ayers & Sun, 1973) the 1989 Loma Prieta (Earthquake Spectra, 1990) and the 1994 Northridge (Earthquake Spectra, 1995) earthquakes have demonstrated the seismic vulnerability of elevator systems. A common elevator damage is the derailment of counterweights. For example, a total of 674 counterweights were reported to have come out of their guide rails in the San Fernando earthquake. There were 10 reports of guide rail anchorage failures, involving anchor bolts being pulled out from hoistway walls. Most of the damage to elevator cars was mainly due to impact with derailed counterweights. The San Fernando earthquake caused 109 cases of such damage. In the Loma Prieta earthquake approximately 1300 elevators were damaged. The Northridge earthquake caused 688 counterweights to come out of their guide rails. It is interesting to note that in spite of the upgrading, in 1980, of existing elevators, and the design of new ones more conservatively, the Northridge damage reports clearly show the need for improving earthquake resistance of elevator counterweight systems and for evaluating the code provisions for elevators and modifying them appropriately so as to accommodate future earthquakes safely. Levy *et al.* (1996) addressed Appendix F of the Safety Code for Elevators and Escalators (ASME

A17.1-1990) and showed that the code could be unconservative by as much as 500% for low buildings and about 50% for tall buildings in Zone 4.

Schiff et al. (1980) and Yang et al. (1983) studied the nonlinear dynamic response of an experimental elevator counterweight model using the finite element method. Tzou and Schiff (e.g. 1989) modeled contact by nonlinear stiffnesses and polynomial damping functions. These studies used sinusoidal base excitation applied to simply supported beams that model the rails. In their model Segal *et al.* (1996) used nonlinear contact elements with air gaps between the counterweight and guide rail support and represented the counterweight subsystem as two concentrated masses at upper and lower shoes levels. An extended model that includes the distributed mass of the counterweight and the stiffness coupling due to the continuity of the rails is used in this paper with real earthquake time histories.

DYNAMIC MODEL OF STRUCTURE-COUNTERWEIGHT SYSTEM

The system model includes the building structure, as a basic independent subsystem, and the counterweight with its rails as a secondary subsystem. This paper considers only counterweight models and their rails, under dynamic excitation. The basic physical models may also apply to a car and its rails.

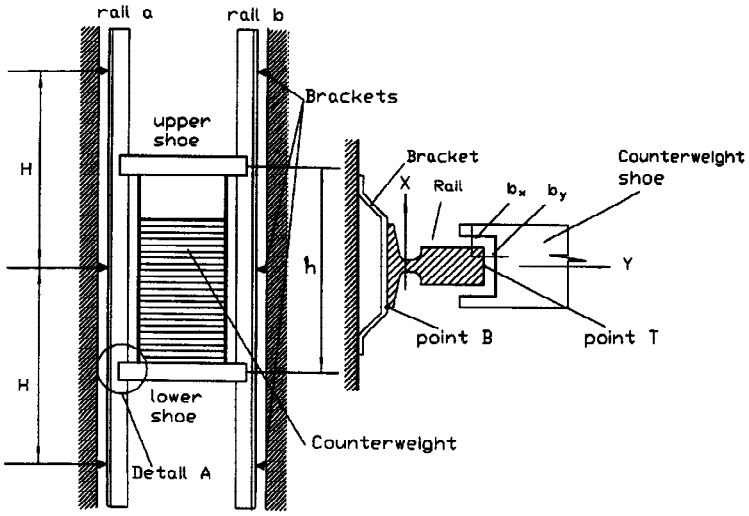

Fig. 1. Counterweight-rail system with detail

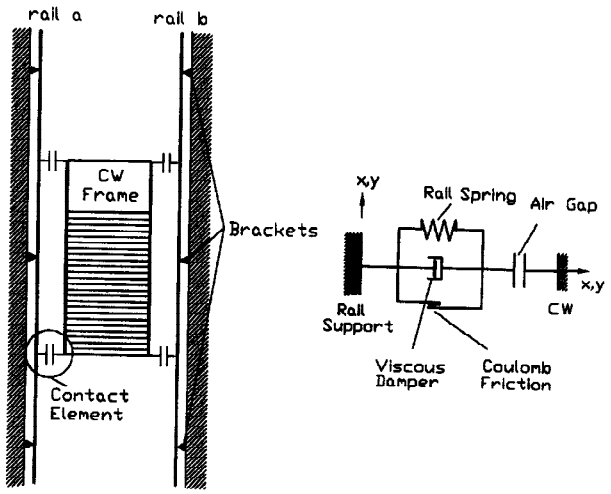

Fig 2. Counterweight model with contact element

Figures 1 and 2 show schematics of the rail-counterweight system. Rails rigidly connect to the structure at close equal intervals and, therefore, experience practically the same lateral displacements as the structure itself. During vertical motion the counterweight swings into contact with one rail in the in-plane direction and with two rails in the out of plane direction. Contact may occur (in both directions) at four points which are the tips of the counterweight frame. The counterweight mass is assumed distributed with generalized coordinates as the contact points. Contact is modeled using the contact element of Fig. 2. Each contact element consists of a spring (rail and/or brackets flexibility), a damper (rail and shoes), Coulomb friction (shoes and/or rail contact surfaces) and two air gaps (clearances).

Dynamic Model of Structure

The generalized equations of motion can be written as:

$$\ddot{X}_i(t) + 2\zeta_s \omega_{x,i} \dot{X}_i(t) + \omega_{x,i}^2 X_i(t) = -\Gamma_{x,i} \ddot{X}_0(t) \qquad (1)$$

$$\ddot{Y}_i(t) + 2\zeta_s \omega_{y,i} \dot{Y}_i(t) + \omega_{y,i}^2 Y_i(t) = -\Gamma_{y,i} \ddot{Y}_0(t) \tag{2}$$

in which $X(t)$, $Y(t)$ = modal displacements of the structure in the i-th mode; ζ_s = viscous damping ratio of structure; $\omega_{x,i}, \omega_{y,i}$ = natural frequencies; $\Gamma_{x,i}, \Gamma_{y,i}$ = modal participation factors; $\ddot{X}_0(t), \ddot{Y}_0(t)$ = base accelerations. $\ddot{X}_0(t), \ddot{Y}_0(t)$ have been chosen for each loading case as follows: $\ddot{X}_0(t) = C\ddot{U}(t)$, $\ddot{Y}_0(t) = C\ddot{V}(t)$ in which C = scaling factor; $\ddot{U}(t), \ddot{V}(t)$ = earthquake ground acceleration for the two horizontal axes.

The horizontal deflection, x_z, and velocity of the structure at any vertical position, z, are obtained from the first mode shape of a flexural cantilever beam which is believed to give sufficiently accurate results.

As the counterweight moves vertically during the earthquake the amplitude of the horizontal motion of the building at the levels of the shoes changes with height and reaches its maximum value at the top of the building. Therefore, the excitation of the counterweight also changes. In order to simplify the analysis it was conservatively assumed that all brackets move horizontally in unison and their motion is equal to the motion of the bracket at the top of the building. Note that the rail stresses due to the deflected shape of the structure itself were found to be relatively small and are therefore neglected in the present study.

Interaction Forces between Counterweight and Guide Rails

The guide rails interaction force vectors that are generated by the counterweight are obtained from the guide rail stiffness matrix and the deflection vector as: $\mathbf{R_x} = \mathbf{K_x u_x}$; and $\mathbf{R_y} = \mathbf{K_y u_y}$; where $\mathbf{R_x}, \mathbf{R_y}$ = interaction force vectors in the x and y directions respectively; $\mathbf{K_x}$, $\mathbf{K_y}$ are the 2×2 stiffness matrices of the subsystem and $\mathbf{u_x}$, $\mathbf{u_y}$ = vectors of guide rail deflections. The guide rail deflection in the x direction of the upper shoe level, $u_{x,1}$, is written as:

$$u_{x,1} = \frac{1}{2}\left[sign\left(x_1 - x_{z,1}\right)\right]\left(\left|x_1 - x_{z,1}\right| - b_x\right)\left[1 + sign\left(\left|x_1 - x_{z,1}\right| - b_x\right)\right] \tag{3}$$

in which $u_{x,1}$ = displacement of counterweight relative to ground and b_x = air gap. The rest of the displacements are obtained by appropriate permutations of x with y and the subscript *1* with *2*.

The stiffness matrices are obtained from the inverse of a 2×2 flexibility matrix whose elements are the flexibilities of the rail modeled as an endless continuous beam on simple supports and the rail bracket flexibilities. For uniformity of results the flexibilities of intermediate spans are considered in this paper for the range of all velocities considered, *0 m/sec.-10.0 m/sec.* Note that because of the automatic stopping, the counterweight cannot be located at the first two spans (which are somewhat more flexible) for speeds higher than *3.0 m/sec.* Following are the intermediate span flexibilities assuming that upper and lower shoes are located at consecutive spans, since the distance between them is usually larger than the distance between the supporting brackets:

$$\delta_{11} = \delta_{11}^0 + \delta_{11}^* = \delta_{11}^0 + \bar{z}_1^2\left(1 - \bar{z}_1\right)^2\left[\frac{\sqrt{3}}{4} + \frac{\bar{z}_1(1 - \bar{z}_1)}{(1 + \sqrt{3})}\right]\frac{H^3}{3EI} \tag{4}$$

$$\delta_{22} = \delta_{22}^0 + \delta_{22}^* = \delta_{22}^0 + \bar{z}_2^2\left(1 - \bar{z}_2\right)^2\left[\frac{\sqrt{3}}{4} + \frac{\bar{z}_2(1 - \bar{z}_2)}{(1 + \sqrt{3})}\right]\frac{H^3}{3EI} \tag{5}$$

$$\delta_{12} = \delta_{12}^0 + \delta_{12}^* = \delta_{12}^0 + \frac{\sqrt{3}\bar{z}_1\bar{z}_2}{(1+\sqrt{3})^4}(1-\bar{z}_1)(1-\bar{z}_2)\left[1+(1+\sqrt{3})\bar{z}_1\right]\left[1+(1+\sqrt{3})(1-\bar{z}_2)\right]\frac{H^3}{3EI} \tag{6}$$

where $\delta_{11}^*; \delta_{22}^*$ = elastic flexibilities of guide rail at the upper and lower contact points; δ_{12}^* = coupled elastic flexibility of guide rail; $\delta_{11}^0; \delta_{22}^0; \delta_{12}^0$ = rail bracket and guide shoes flexibilities; $EI = EI_x$ or $2EI_y$ = flexural rigidities of the rail; H= rail span; $\bar{z}_j$ = guide shoe relative position along the rail within a particular span, and is obtained from $\bar{z} = \left(z_j / H\right) - n$, where z_j = current position of upper j= *1*, and lower j= *2* contact point, i.e. $z_1 = z_0 + vt$; $z_2 = z_1 - h$; z_0 = initial position of upper contact point assumed at roof level measured from the base; v= vertical velocity of counterweight; h= distance between guide shoes and n= number of spans below the current span.

Dynamic Model of Counterweight

A linear contact element with viscous damping and Coulomb friction is proposed to model dynamic interaction between the structure and the elevator subsystems. Coulomb's friction is activated only when biaxial excitation is present in which case the interaction force in the x direction restraints motion in the y direction and vice versa.

The generalized differential equations of the counterweight motion can be written as:

$$\left[\mathbf{M_x}\right]\{\ddot{\mathbf{x}}\} + \left[\mathbf{C_x}\right]\{\dot{\mathbf{u}}_\mathbf{x}\} + \left[\mathbf{K_x}\right]\{\mathbf{u_x}\} + \mu_x\{\mathbf{R_y}\} = -\ddot{X}_0\left[\mathbf{M_x}\right] \tag{7}$$

$$\left[\mathbf{M_y}\right]\{\ddot{\mathbf{y}}\} + \left[\mathbf{C_y}\right]\{\dot{\mathbf{u}}_\mathbf{y}\} + \left[\mathbf{K_y}\right]\{\mathbf{u_y}\} + \mu_y\{\mathbf{R_x}\} = -\ddot{Y}_0\left[\mathbf{M_y}\right] \tag{8}$$

The mass matrix in the general coordinates (shoe levels) is given as:

$$\mathbf{M} = \mathbf{A}^\mathbf{T}\mathbf{m}\mathbf{A} = \begin{bmatrix} 1-\frac{a}{2h} & \frac{1}{h} \\ \frac{a}{2h} & -\frac{1}{h} \end{bmatrix}\begin{bmatrix} m & 0 \\ 0 & J \end{bmatrix}\begin{bmatrix} 1-\frac{a}{2h} & \frac{a}{2h} \\ \frac{1}{h} & -\frac{1}{h} \end{bmatrix} = \begin{bmatrix} (1-\frac{a}{2h})^2 m + \frac{J}{h^2} & \frac{a}{2h}(1-\frac{a}{2h})m - \frac{J}{h^2} \\ \frac{a}{2h}(1-\frac{a}{2h})m - \frac{J}{h^2} & \frac{a^2 m}{4h} + \frac{J}{h^2} \end{bmatrix} \tag{9}$$

Here **M**, **m** and **A** are the generalized mass matrix, the primitive mass matrix and the transformation matrix respectively; m is the counterweight mass; J is the mass moment of inertia; h is the distance between contact points and a is the height of the distributed mass. The familiar Rayleigh damping matrices are assumed, i.e.

$$\mathbf{C_x} = a_{x0}\mathbf{M_x} + a_{x1}\mathbf{K_x}, \qquad \mathbf{C_y} = a_{y0}\mathbf{M_y} + a_{y1}\mathbf{K_y}, \qquad a_{x0} = 2\xi_x\frac{\bar{\omega}_{x1}\bar{\omega}_{x2}}{\bar{\omega}_{x1}+\bar{\omega}_{x2}}; \qquad a_{x1} = 2\xi_x\frac{1}{\bar{\omega}_{x1}+\bar{\omega}_{x2}};$$

$\xi_x = \frac{a_{x0}}{2} + \frac{a_{x1}\omega_n}{2}$, where ξ_x is the damping ratio and $\bar{\omega}_{x1}; \bar{\omega}_{x2}$ are the natural frequencies of the counterweight-guide rail subsystem in the x direction and are determined by solving the eigenvalue equation $\left|\mathbf{K_x} - \bar{\omega}_x^2\mathbf{M_x}\right| = \mathbf{0}$. Equations 7 and 8 are coupled through mass, stiffness and friction. Stiffness coupling arises through the continuity of the rail. (A force at one shoe level leads also to a deflection at the other level.) Mass coupling arises since the counterweight may rotate as a rigid body mobilizing its moment of inertia.

In-plane motion (Eq. 7) makes both rails work. In a given direction the gap is first closed when the rail is pushed in that direction by the counterweight. When the gap opens and the second rail is activated, a new negative cycle has begun since the two rails are identical. So for the in-plane rail direction (axis y) in each time step the signs of the guide rail deflections in upper and lower points are checked. When the signs are opposite

(at one point the counterweight touches guide rail *a* (Fig. 1) and at another guide rail *b*) coupling stiffness is taken as zero and Eqs. 7, 8 are calculated over again.

At this stage Eqs. 1 and 2 are each expanded into *2* differential equations of the first order (*2* for each of the first flexural normal mode of a distributed parameter model) and Eqs. 7 and 8 are each expanded into *4* differential equations of the first order (*2* for each of the two degrees of freedom at each contact point) for a total of *12* differential equations. These are solved using the Runge-Kutta fifth order method from the IMSL library of routines called from a FORTRAN coded main program to yield structure and counterweight displacements relative to the ground. With these displacements at hand maximum guide rail interaction forces and maximum guide rail moments and maximum stresses are extracted at each time instant. The evaluated stresses can be used in the design of rails. The estimation of deflections is necessary to avoid derailment, whereas the interaction forces determine the counterweight frame and shoes details. The guide rail stresses are calculated for the two cross section points T and B (Fig. 2.) considering biaxial bending. Coupling in the stiffness is considered wherever appropriate since contact of upper and lower levels may be at different rails at some specific time.

PARAMETRIC STUDY

The NS and EW components of 1940 El Centro earthquake excitations are used in this study. A first mode frequency, *2.0 Hz,* is assumed for each of the two horizontal axes. The total mass of the counterweight is taken as $m = 1.0$ *ton* with the ratio of 1/2 between the length of weight sections and counterweight frame space. A standard *12 lbs/ft* guide rail is used in this study. The bracket flexibilities are taken as, $\delta_{11}, \delta_{22} = 0.5$ *cm/ton* and $\delta_{12} = 0$. The clearance (air gap) between the guide shoes and rail is $b = 0$ or *2 mm*. Viscous damping for the structure is assumed to be $\xi = 5\%$ for concrete (the structure) and $\xi = 2\%$ for steel (the guide rail). A Coulomb friction at *17%* is introduced into the contact elements.

Effect of Vertical Velocity

Results of numerical analyses were compiled for a range of elevator velocities, *0 - 10.0 m/sec* and for two clearances (air gaps) values of *0.0 mm* and *2.0 mm.* in terms of maximum guide rail deflections, interaction forces and stresses. Displayed, however, are results for stresses only. Figure 3 shows two curves which are obtained using the initial condition of $z_0 = H/2$ (z_0= location of the upper shoe). The heavy line curve displays the results of the described model, and the dotted curve shows the results of the model of Segal *et al.* (1996). The results clearly demonstrate the dependence of the response on the vertical velocity of the counterweight, and the modeling method. Several effects are noticeable. The wavy quasi harmonic deflection curves may be deceptive since it stems from the fact that the maximum response for different vertical velocities occurs at different mass locations with respect to the rail supports to result in different effective rail stiffness. A true maximum response at a given velocity may be obtained by continuously varying the initial location of the counterweight (z_0) along the span length. Figure 4 shows the results for the combined effect of four initial positions of upper counterweight shoes in the case without gaps. The envelope can be obtained by connecting all the peaks.

The increase in response with increasing vertical velocity can be attributed to the effect of centrifugal forces resulting from the deflection curve. A comparison of the stress response of a *22 lb* rail with the stress response of a *12 lb* rail results in that the effect of centrifugal force decreases with increasing guide rail stiffness in proportion to the ratio of the moments of inertia of the two guide rails. It is appropriate to mention here that since, for low elevator velocities, the counterweight may be positioned at the first and second spans which are more flexible a somewhat larger response is expected. For more details the reader is referred to Marianchik (1996).

EVALUATION OF ELEVATORS SAFETY SEISMIC PROVISIONS

This section specifically addresses Appendix F of the Safety Code for Elevators and Escalators (ASME A17.1-1990) by presenting a modified version for one of the charts (Figs. F200.4c(1)-(7)): that of Fig. F200.4c(3), (*12 lb* Guide-Rail Bracket Spacing) with no intermediate tie brackets for seismic risk Zone 4. It provides two charts. One with an air gap of *2.0 mm* and another without air gaps, each of which contains curves for buildings with fundamental periods of *0.5 secs, 1.0 sec* and *2.0 secs*. Each figure in Appendix F of the code is dedicated to a specific guide rail weight, covering *8 lb, 11 lb, 12 lb, 15 lb, 18.5 lb, 22.5 lb* and *30 lb* guide rails. The ordinates in these figures are the maximum permissible weight of the counterweight in *kips* for a given bracket spacing in *ft* as the abscissas. All the charts in that Appendix are for seismic Zone 3 or higher. Each point on the design charts was obtained by performing a complete dynamic analysis as described in the previous sections, iteratively, as the counterweight mass was redesigned to produce allowable levels of guide rail stresses. The total mass of the counterweight was taken as *m=1.5 ton* with the weight sections taking two thirds of the length of the counterweight frame.

As for the actual earthquake motion, a set of *26* earthquake records carefully grouped in bidirectional pairs according to their ratio of peak ground acceleration (PGA) to peak ground velocity (PGV), the A/V ratio, was extracted from Naumoski et al (1993). These were scaled to PGV of *0.4 m/sec* and used as excitations to produce stresses which were statistically evaluated and compared with the design charts of Appendix F of the code. (Levy et al. 1996). It is appropriate to note that since the UBC zones are classified on the basis of PGA (or in fact on its effective value (EPA), which is somewhat lower) rather than on PGV with a design spectrum which is close to the A/V=1 spectrum, the response of sites with A/V<1 is underestimated and A/V>1 is overestimated by the PGV scaling.

Design Chart

Appendix F of the safety code for elevators and escalators (ASME A17.1-1990) requires that "stresses in a guide rail, or in the rail and its reinforcement, due to the horizontal forces imposed on the rail by a seismic force of not less than that required to produce an acceleration of 1/2 gravity acting horizontally on the car with 40% rated load, or the counterweight, shall not exceed 88% of the minimum yield stress of the material used". The guide rails are made of steel having a yield stress of *36,000 psi* (*248 MPa*), so the maximum permissible stress in the guide rail due to seismic horizontal forces is $\sigma=248*0.88=218\ MPa$, which is the stress level used for constructing the design charts. The recurrence relationship for the iterative procedure that is used to obtain the maximum permissible weight of the counterweight for a given bracket spacing may be written as $WT^{(n+1)} = WT^{(n)}\left(\sigma_{allowable} / \sigma^{(n)}_{calculated}\right)$ where $WT^{(n)}$ is the weight of the counterweight in the n-th iteration, $\sigma^{(n)}_{calculated}$ is the calculated stress on the guide rails at the n-th iteration and $\sigma_{allowable}$ is the allowable stress which has been set at *218 MPa*. As noted, the records were scaled to PGV = *0.4 m/sec* (for Zone 4 design) and the mean minus one standard deviation results for all of the *26* records were calculated without differentiating among A/V levels and displayed in Figs. 5,6 for zero and *2.0 mm* gaps respectively.

CONCLUSIONS

In this study the earthquake response of a structure-counterweight system with nonlinear contact elements under seismic excitation is studied and evaluated. The contact forces and stresses within the rail depend on the mass of the counterweight, the width of the gap, the geometry of the rail section, span between brackets, the guide rail stiffness, natural period, deflected shape of the structure and on the intensities of the earthquake excitation. Dynamic contact between the counterweight and the guide rails can induce large forces that endanger the elevator systems. The effect of velocity manifests itself mainly in the variable stiffness of the rail. The peak response depends on the vertical location of the counterweight at maximum excitation of the

earthquake. Also, increasing the vertical velocity increases the peak response. Since this increase depends on the centrifugal force, a larger rail stiffness will have a reducing effect. The response of the system also depends on the natural frequency of the structure. For the same dynamic parameters of the structure-counterweight system and earthquake excitation, the rail deflection, the interaction forces, and the stresses increase with decreasing of the natural period of the structure and reach its maximum at resonance. The maximum design weight of the counterweight, thus, depends on the natural period of the structure. As expected, increasing the bracket spacing leads to a reduction of the permissible suspended counterweight mass.

At practical bracket spacings (*8-12 ft*) the proposed model predicts the code to be unconservative by as much as ***500%*** for low buildings and about *50%* for tall buildings.

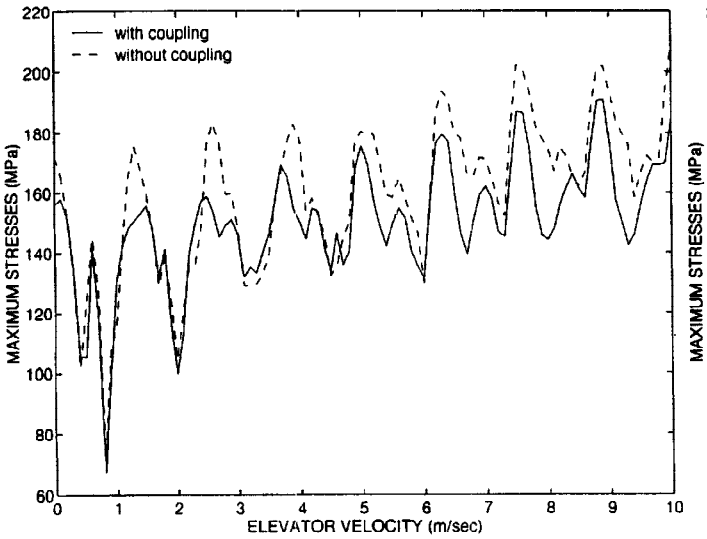

Fig.3. Maximum rail stresses (gap=0 mm)

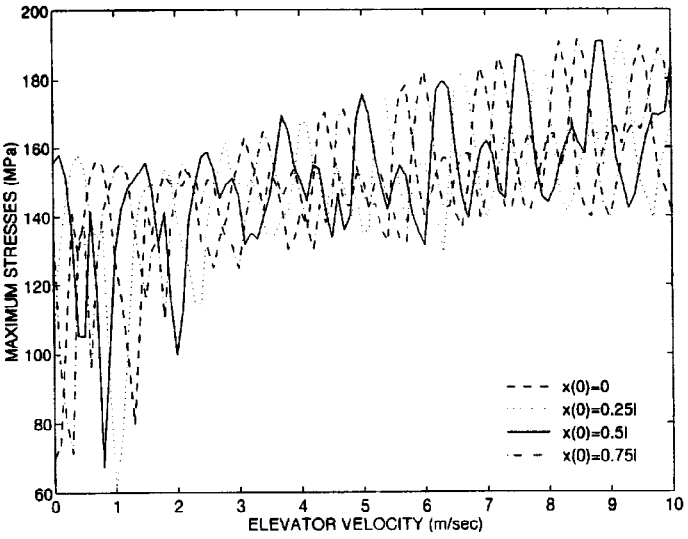

Fig. 4.Maximum rail stresses. Four initial locations (gap=0 mm)

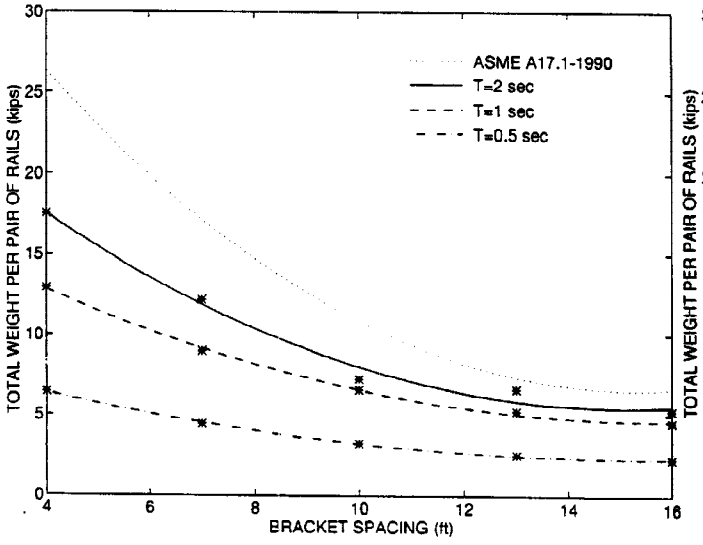

Fig. 5.Total weight vs. rail bracket spacing. Zone 4, 26 records (gap=0 mm)

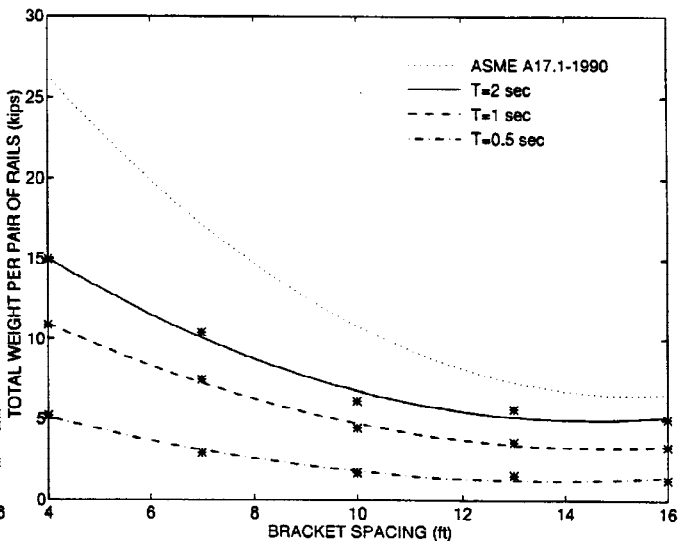

Fig. 6.Total weight vs. rail bracket spacing. Zone 4, 26 records (gap=2 mm)

REFERENCES

ASME, (1991), Safety Code for Elevators and Escalators ASME, A17-1990, Appendix F, The American Society of Mechanical Engineers, New York, NY 10017, 309-328.

Ayers, J. M. and Sun, T.-Y., (1973), Nonstructural Damage, San Fernando, California, Earthquake of February 9, 1971, Part B, U. S. Dept. of Commerce, NOAA, Washington, D.C., Vol. 1, 735-776.

Ayres, J. M., Sun, T.-Y. and Brown, F.R., (1973), Nonlinear Damage to Buildings, The Great Alaska Earthquake of 1964, Engineering. National Academy of Sciences, Washington, D.C.

Earthquake Spectra (1990) Loma Prieta Earthquake Reconnaissance Report, , Supplement to Vol. 6, 364 - 376.

Earthquake Spectra (1995) Northridge Earthquake of January 17, 1994 Reconnaissance Report, Volume 1, (John F. Hall, editor), supplement to Vol. 11, publication 95-03, pp. 468

Levy, R., Rutenberg, A., Segal, F. and Marianchik, E., (1996) "Analytical Evaluation of Elevators Safety Code Seismic Provisions", *Elevator World*, (to be published).

Marianchik, E.,(1996) Dynamic Analysis and Design of Elevator Counterweight Guide Rails for Earthquakes M.Sc. thesis, Department of Civil Engineering Technion - Israel Institute of Technology, Haifa.

Naumoski, N., Heidebrecht, A.C., and Rutenberg, A., (1993), Representative Ensembles of Strong Motion Earthquake Records, EERG Report 93-1, Earthquake Engineering Research Group, McMaster University, Hamilton, Ontario.

Schiff, A. J., Tzou, H. S. and Chu, Y.H., (1980), "Earthquake response of elevator counterweights," *Proc. of the 7th World Conference on Earthquake Engineering*, Vol. 8, Istanbul, 483-486.

Segal, F.R., Rutenberg, A. and Levy, R., "Earthquake Response of Structure-Elevator Systems," *Journal of Structural Engineering*, ASCE, 1996, (to be published).

Tzou, H. S. and Schiff, A. J., (1989), "Dynamics and Control of Elevators with Large Gaps and Rubber Dampers," *Journal of Structural Engineering*, ASCE, Vol. 115, No. 11, 2753-2771.

Yang, T.Y., Kullegowda, H., Kapinia, R.K. and Schiff, A.J., (1983), "Dynamic Response Analysis of Elevator Model," *Journal of Structural Engineering*, ASCE, Vol. 109, No. 5, 1194-1210.